

Letter of Intent to JLab PAC51

Study of charge symmetry breaking in p-shell hypernuclei

T. Gogami,^{1,*} F. Garibaldi,^{2,3} P. Markowitz,⁴ J. Reinhold,⁴ S. Nagao,⁵
S. N. Nakamura,⁵ B. Pandey,⁶ L. Tang,^{7,8} and G. M. Urciuoli²

(on behalf of JLab Hypernuclear Collaboration)

¹*Department of Physics, Graduate School of Science, Kyoto University, Kyoto, Kyoto 606-8502, Japan*

²*INFN, Sezione di Roma, 00185 Rome, Italy*

³*Istituto Superiore di Sanità, 00161 Rome, Italy*

⁴*Department of Physics, Florida International University, Miami, FL 33199, USA*

⁵*Graduate School of Science, The University of Tokyo, Tokyo 113-0033, Japan*

⁶*Department of Physics & Astronomy, Virginia Military Institute, Lexington, Virginia 24450, USA*

⁷*Department of Physics, Hampton University, Hampton, VA 23668, USA*

⁸*Thomas Jefferson National Accelerator Facility (JLab), Newport News, VA 23606, USA*

(Dated: May 22, 2023)

One of important features in the ΛN interaction is charge symmetry breaking (CSB). Firm evidence of CSB was found in a binding-energy difference for s-shell iso-doublet Λ hypernuclei, ${}^4_{\Lambda}\text{He}$ and ${}^4_{\Lambda}\text{H}$. The origin of CSB is an open question, and it is obvious that data for the other hypernuclear systems are indispensable. Therefore, studies in the p-shell hypernuclei attract a strong interest to pin down the origin of CSB. Accurate data with the uncertainty of less than about 100 keV are necessary because the CSB effect in the p-shell hypernuclei are expected to be smaller than that in the s-shell system. A total of 516 hours (21.5 days) of beam time allows us to investigate the CSB effect for the mass number of $A = 6, 9,$ and 11 with the world's best accuracy $|\Delta B_{\Lambda}^{\text{total}}| = 70$ keV. This proposed experiment aims to complete the accurate data set for the p-shell hypernuclei up to the mass number of twelve by a collaborative experimental research with the hadron-beam facility at J-PARC, Japan.

* Contact person, gogami.toshiyuki.4a@kyoto-u.ac.jp / gogami@jlab.org

EXECUTIVE SUMMARY

A beam condition and an experimental setup at Hall C are the same as those for approved hypernuclear experiments E12-15-008 and E12-20-013. Electron beams at the energy of $E_e = 2.24$ GeV and the intensity of $I_e = 50 \mu\text{A}$ are impinged on isotopically enriched targets (${}^6\text{Li}$, ${}^9\text{Be}$ and ${}^{11}\text{B}$) with the areal density of 100 mg/cm^2 . Scattered electrons and K^+ 's generated from the ${}^6\text{Li}(e, e'K^+)_{\Lambda}{}^6\text{He}$, ${}^9\text{Be}(e, e'K^+)_{\Lambda}{}^9\text{Li}$, and ${}^{11}\text{B}(e, e'K^+)_{\Lambda}{}^{11}\text{Be}$ reactions are measured by existing spectrometers HES and HKS for which central momenta were set to 0.74 and 1.2 GeV/ c , respectively. Energy-calibration data of E12-15-008, Λ and Σ^0 productions from a polyethylene target, are commonly used. Therefore, the beam time for only the physics runs is requested herewith. A total of the requesting beam time is 516 hours (21.5 days).

I. INTRODUCTION

A. To study the bayron-baryon interaction

Hypernuclear spectroscopy is the most important tool to investigate the baryon-baryon (BB) interaction with strangeness degrees of freedom ($S < 0$). In the non-strangeness sector ($S = 0$), there are rich data of scattering and spectroscopic experiments. More than 3000 species of nuclei have been experimentally identified. In the $S < 0$, on the other hand, data from the scattering experiment are extremely scarce due to technical issues related to the short lifetimes of hyperons. In addition, the number of hypernuclear species which were measured so far is only about 40. A scattering experiment between proton and $\Sigma^{+, -}$ had been successfully performed at J-PARC recently [1, 2]. CLAS collaboration also reported the measurement of scattering between proton and Λ [3]. Future programs for the hyperon-nucleon (YN) scattering experiment are planned at J-PARC and expected to provide significant information on the YN interaction [4].

The importance of the hypernuclear spectroscopy would be further emerged when the future YN scattering experiments are realized. The better understanding of the YN interaction would lead to better understanding of such as a many-body force from the hypernuclear structures. The many-body force should play an important role in dense nuclear matter such as neutron stars. There are arguments that only the two-body ΛN force cannot support the existence of two-solar mass neutron stars which were observed, but an inclusion of the three-body repulsive force YNN. Also, ΛNN repulsive interaction may cause to suppress the generation of Λ in the neutron stars, leading to an allowance of the existence of two-solar mass neutron stars in calculations. To investigate the ΛNN three-body force, we plan to precisely measure the hypernuclear energies of ${}_{\Lambda}^{40,48}\text{K}$ (JLab E12-15-008) [5] and ${}_{\Lambda}^{208}\text{Tl}$ (JLab E12-20-013) [6].

An important feature of the ΛN force is the ΛN - ΣN coupling. The ΛN - ΣN coupling is expected to be an origin to cause the charge symmetry breaking (CSB) in the ΛN interaction. The ΛN CSB was found in the binding-energy difference between ${}_{\Lambda}^4\text{He}$ and ${}_{\Lambda}^4\text{H}$ hypernuclei [7–9]. To confirm the data for the CSB study in the $A = 4$ system by modern experimental techniques, we are going to perform JLab E12-19-002 experiment in which ${}_{\Lambda}^4\text{H} (J^{\pi}; 1^+)$ is planned to be measured with the world's best accuracy [10–12]. J-PARC E63 is also going to measure the same state by the γ -ray spectroscopy at J-PARC [13, 14]. The γ -ray spectroscopy measures γ rays from de-excitation processes of various energy states. Therefore, the γ -ray spectroscopy measures the excited energies, and it needs the ground state information to determine the absolute energy, which

is from independent experiments in this case, to determine the absolute energy. On the other hand, JLab E12-19-002 measures the 1^+ state in ${}^4_{\Lambda}\text{He}$ directly. Therefore, the missing mass spectroscopy at JLab and the γ -ray spectroscopy are complementary, and will pin down the CSB effect in the $A = 4$ hypernuclear system. CSB in the p-shell hypernuclear system was studied at JLab by measuring ${}^7_{\Lambda}\text{He}$ [15, 16] and ${}^{10}_{\Lambda}\text{Be}$ [17]. The total error on the binding energy, that takes statistical and systematic errors into account, was $|\Delta B_{\Lambda}^{\text{total}}| \simeq 150$ keV. In this proposed experiment, ${}^6_{\Lambda}\text{He}$, ${}^9_{\Lambda}\text{Li}$, and ${}^{11}_{\Lambda}\text{Be}$ are aimed to be measured with an improved accuracy of $|\Delta B_{\Lambda}^{\text{total}}| = 70$ keV which is the world's best accuracy among existing reaction spectroscopy. The accurate hypernuclear measurement which we propose here will lead to a completion of the data set for discussing CSB up to the mass number $A = 12$.

B. Comparison with other experiments

Missing-mass spectroscopy of Λ hypernuclei at JLab has been playing an indispensable role in the strangeness nuclear physics. Uniqueness of the JLab's hypernuclear project has roots in the best resolution and accuracy in a resulting missing-mass spectrum. The resolution and accuracy that we have achieved at JLab are 0.5 MeV (FWHM) and $|\Delta B_{\Lambda}^{\text{total}}| \sim 0.1$ MeV, respectively. They are better by a factor of 3–5 compared to the best resolution and accuracy obtained in the past experiments by hadron beams at KEK, Japan [18]. The missing-mass spectroscopy is applicable for light to heavy mass systems although other experimental techniques are limited to the light mass systems as shown in this section.

1. Nuclear emulsion experiment

The nuclear emulsion experiment measures Λ binding energy with the accuracy as good as a few 10 to 100 keV up to the mass number of $A = 19$ [19, 20]. Most of Λ hypernuclei generated in emulsion plates are de-excited to the ground state before their weak decays to be observed as tracks. Therefore, the emulsion experiment determines the ground-state energies of Λ hypernuclei for the most cases. The accurate measurement is possible by the emulsion technique particularly for hypernuclear species which have large statistics. However, one should note that hypernuclei with low statistics may have an additional systematic error due to a difficulty of unique identification of signals in image analysis processes. For example, the binding energy of ${}^{12}_{\Lambda}\text{C}$, for which less than 10 events were identified, is found to be shifted by 0.5–0.6 MeV [17, 21].

2. γ -ray spectroscopy

The γ -ray spectroscopy with Ge detectors has much better resolution, which is a few keV, and successfully measured low-lying hypernuclear structures up to the mass number of $A = 19$ [22]. The γ -ray spectroscopy measures energy spacings between particular states, which means it does not measure the absolute energy. On the other hand, the missing mass spectroscopy at JLab has an advantage in measuring the absolute energy due to a calibration by using Λ and Σ^0 productions from a proton target [23, 24].

3. Decay π spectroscopy

The decay π spectroscopy in which two-body weak decays of hypernuclei at rest are measured is one of the most accurate ways to determine the binding energy of Λ hypernuclei. It is noted that only ground-state energies are measurable by this method. It measures π^- 's with the momentum of the order of 100 MeV/c, and thus a spectrometer with $\Delta p/p = 10^{-4}$ (FWHM) can achieve more precise energy resolution by an order of magnitude than that in the missing-mass spectroscopy at JLab. The experimental technique had been proven at MAMI by measuring the ground-state energy of ${}^4_{\Lambda}\text{H}$ from a ${}^9\text{Be}$ target [7, 8]. As a new attempt, the experimental target was changed to ${}^7\text{Li}$, to measure the ground-state energy of hypertriton ${}^3_{\Lambda}\text{H}$ [25]. In addition, the the calibration method by using undulators will be adopted to improve the systematic error down to only about 20 keV [26, 27]. The data taking for the hypertriton measurement was performed at MAMI in 2022. In the fall of 2023, the beam-energy calibration with the new undulators is planned to be carried out. Experimental performance of the the decay π spectroscopy is expected to be improved at JLab as described in LoI which we independently submitted to this PAC.

The approved experiment JLab E12-19-002 also aims to measure the hypertriton's binding energy by the missing-mass spectroscopy [10]. The accurate measurements from the different experimental techniques are of great importance to confirm the experimental data. In addition, E12-19-002 would be able to observe and determine the first excited state ($3/2^+$) for the first time, instead of the ground state ($1/2^+$) if it exists. So far, the measurement of the excited state of hypertriton is possible at only JLab. The existence of the $3/2^+$ state is an open question, and the data would be one of fundamental information for constructing the ΛN interaction particularly for the spin-triplet interaction.

4. Heavy-ion beam experiment

In experiments of heavy-ion beams on a fixed target [28] and heavy-ion collisions [29–31], the Λ -binding energies of Λ hypernuclei for the $A = 3$ and 4 were measured. Important feature of the experiment is that they could observe anti-hypernuclei as well. Also, the heavy ion experiment can measure the lifetimes of hypernuclei.

As for the YN and YY interaction studies, a new experimental technique so called femtoscopy was proved to be possible and in fact quite powerful [32, 33]. The femtoscopy measures relative momentum distributions for particular two particles of interest. The relative momentum distribution contains the information of the interaction of the particles. New experimental data are promising and awaited. However, a question is how to derive the spin dependent integration from the femtoscopy, and so far, only the spin-averaged interaction is discussed.


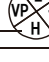
5. Missing-mass spectroscopy by hadron beams

The missing-mass spectroscopy by using (π^+, K^+) and (K^-, π^-) reactions are typical reaction spectroscopy by hadron beams. These hadron beam reactions convert a neutron into a Λ . On the other hand, the $(e, e'K^+)$ reaction which is used at JLab converts a proton into a Λ . Therefore, hypernuclei that have different isospins can be investigated from the same experimental target by using the hadron and electron beams. In particular, mirror hypernuclei can be generated by choosing appropriate targets. The resolution and accuracy in the hadron-beam spectroscopy was limited in the past experiment at CERN, BNL and KEK. In 2022, a new magnetic spectrometer S-2S [34, 35] which is dedicated to measure hypernuclei was constructed and successfully installed in the K1.8 beam line of the Hadron Experimental Facility of J-PARC, Japan. The S-2S spectrometer has an excellent momentum resolution of $\Delta p/p = 6 \times 10^{-4}$ in FWHM. The momentum resolution is worse than that of HKS and HES which are spectrometers used in the proposed experiment. However, the (π^+, K^+) experiment using S-2S is expected to achieve 1-MeV resolution (FWHM) in a resulting energy spectrum. Such a high resolution allows an experiment to use better calibration sources than the binding energy of ${}_{\Lambda}^{12}\text{C}$ which was the only choice to be used in the past experiments with the (π^+, K^+) reaction. There is an argument that the measured energy of ${}_{\Lambda}^{12}\text{C}$ has the energy shift of about 0.5 MeV, leading to a systematic error on the measured hypernuclear energies. Now, there is a plan to use the binding energies of $3/2^+$ and $5/2^+$ states of ${}_{\Lambda}^7\text{Li}$ for the absolute energy calibration in the (π^+, K^+) experiment (J-PARC E94) [36]. The high energy resolution allows one

to distinguish the $3/2^+$ and $5/2^+$ states which could not be separated in the missing-mass spectrum of the past experiments. The expected accuracy is about $|\Delta B_{\Lambda}^{\text{total}}| = 100$ keV which is comparable to the accuracy in the proposed experiment, $|\Delta B_{\Lambda}^{\text{total}}| = 70$ keV. On this context, it is now the time to seriously tackle to find out the origin of CSB by systematically measuring mirror p-shell Λ hypernuclei at JLab and J-PARC.

II. GOAL OF THE EXPERIMENT

We aim to determine the energies of ground-state peaks of ${}^6_{\Lambda}\text{He}$, ${}^9_{\Lambda}\text{Li}$, and ${}^{11}_{\Lambda}\text{Be}$ with the accuracy of $|\Delta B_{\Lambda}^{\text{total}}| = 70$ keV for the study of CSB. Figure 1 shows the isospin multiplet hypernuclei to be compared with each other to test the CSB effect. There are labels, E, VP, γ and H. VP and H

Electron-beam experiment at JLab  Emulsion experiment
 Hadron-beam experiment at J-PARC  γ -ray experiment




















Hypernucleus		CSB study					
		T<0	T=0	T>0	Now	New JLab	J-PARC
s-shell	$d N \Lambda$ (0^+)	${}^4\text{H}$		${}^4_{\Lambda}\text{He}$			
	$d N \Lambda$ (1^+)	${}^4_{\Lambda}\text{H}$		${}^4_{\Lambda}\text{He}$			
p-shell	$\alpha N \Lambda$	${}^6_{\Lambda}\text{He}$		${}^6_{\Lambda}\text{Li}$			
	$\alpha N N \Lambda$	${}^7_{\Lambda}\text{He}$	${}^7_{\Lambda}\text{Li}^*$	${}^7_{\Lambda}\text{Be}$			
	$\alpha d N \Lambda$	${}^8_{\Lambda}\text{Li}$		${}^8_{\Lambda}\text{Be}$			
	$\alpha d N N \Lambda$	${}^9_{\Lambda}\text{Li}$	${}^9_{\Lambda}\text{Be}$	${}^9_{\Lambda}\text{B}$			
	$\alpha \alpha N \Lambda$	${}^{10}_{\Lambda}\text{Be}$		${}^{10}_{\Lambda}\text{B}$			
	$\alpha \alpha N N \Lambda$	${}^{11}_{\Lambda}\text{Be}$	${}^{11}_{\Lambda}\text{B}$	${}^{11}_{\Lambda}\text{C}$			
	$\alpha \alpha d N \Lambda$	${}^{12}_{\Lambda}\text{B}$		${}^{12}_{\Lambda}\text{C}$			

FIG. 1. The table of hypernuclei to study the CSB in the ΛN interaction.

represent the data from the experiments by electron and hadron beams. E is for the data by the emulsion experiment, but the data that have the statistical error of over 100 keV are omitted from the list. γ stands for the data from the γ -ray spectroscopy.

The ground state energies of ${}^9_{\Lambda}\text{Be}$ and ${}^{11}_{\Lambda}\text{B}$ were determined by the emulsion experiment. Therefore, the determination of the energies for ${}^9_{\Lambda}\text{Li}$ and ${}^{11}_{\Lambda}\text{Be}$ hypernuclei by the proposed experiment makes the energy comparison possible to test the CSB effect. On the other hand, ${}^6_{\Lambda}\text{Li}$, which is the isospin partner of ${}^6_{\Lambda}\text{He}$, has not been measured. However, the measurement of the ${}^6_{\Lambda}\text{Li}$ hypernucleus is possibly be done by the future experiment with the (π^+, K^+) reaction at J-PARC. The missing-mass spectroscopy at JLab successfully measured the binding energy of ${}^7_{\Lambda}\text{He}$ [15, 16], ${}^{10}_{\Lambda}\text{Be}$ [17], and ${}^{12}_{\Lambda}\text{B}$ [23]. The CSB effect for $A = 7$ was studied based on the obtained experimental result compared with its iso-multiplet partners. As a result, it confirms that the CSB effect for $A = 7$ is small. Accurate data for ${}^{10}_{\Lambda}\text{B}$ and ${}^{12}_{\Lambda}\text{C}$ are planned to be provided in the J-PARC E94 experiment [36], and the CSB effects in $A = 10$ and 12 will be clarified by a comparison with the data of ${}^{10}_{\Lambda}\text{Be}$ and ${}^{12}_{\Lambda}\text{B}$ which are from JLab. Experimental data for $A = 8$ were already provided by the emulsion experiment.

The data set for the CSB study in the p-shell hypernuclei would be completed by the above strategy. The origin of the CSB is considered to be from the $\Lambda\text{N}-\Sigma\text{N}$ coupling. However, it is still difficult to quantitatively reproduce Λ binding energies of light Λ hypernuclei. The CSB effect has been studied from the hypernuclear energies particularly for $A = 4$ [37, 38]. However, it is obvious that the other data by which the CSB effect would be tested are necessary to pin down the origin of CSB. Therefore, the systematic investigation in the p-shell hypernuclei attracts a strong interest [39–43]. The proposed experiment provides crucial data to complete the data set for the CSB study in the p-shell hypernuclear systems.

III. EXPERIMENTAL SETUP

The experimental setup is the same as that for approved experiments E12-15-008 (${}^{40,48}_{\Lambda}\text{K}$) and E12-20-013 (${}^{208}_{\Lambda}\text{Tl}$). Figure 2 shows a schematic of the experimental setup at Hall C. Existing spectrometers HES and HKS [44–46] are used for e' and K^+ detections, combined with a new pair of charge separation dipole magnets (PCS). The HES and HKS bend particles horizontally. It is noted that, on the other hand, an experimental project with gas targets (E12-19-002, ${}^{3,4}_{\Lambda}\text{H}$) uses a different experimental configuration because it needs at least one vertical bending spectrometer. A construction of PCS was completed by Japanese company TOKIN, and transported to JLab in 2022. All the magnets including PCS are at experimental staging building (ESB), JLab.

One of important features of the spectrometer system is the high energy resolution in a resulting energy spectrum. Momentum resolutions for HES and HKS which are combined with PCS are at

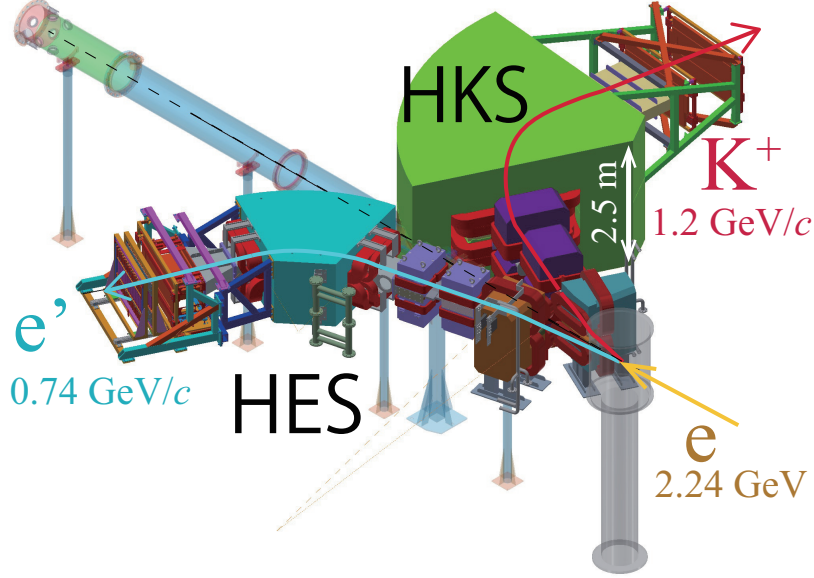


FIG. 2. Schematic of the experimental setup at Hall C. HES and HKS are used for detections of e' and K^+ , respectively. The setup is the same as that for approved experiments E12-15-008 (${}_{\Lambda}^{40,48}\text{K}$) and E12-20-013 (${}_{\Lambda}^{208}\text{Tl}$). The proposed experiment aims to measure neutron rich hypernuclei ${}_{\Lambda}^6\text{He}$, ${}_{\Lambda}^9\text{Li}$, and ${}_{\Lambda}^{11}\text{Be}$.

the level of $\Delta p/p = (2-5) \times 10^{-4}$ in the full width at half maximum (FWHM). The high momentum resolutions lead to the energy resolution of 0.6 MeV in FWHM in the Λ -binding energy spectrum.

A. Kinematics

Electron beams at $E_e = 2.24$ GeV are impinged on an experimental target. Scattered electrons and K^+ 's from the $(e, e'K^+)$ reaction are measured by HES and HKS, respectively. The central momentum of HES is set to 0.74 GeV/c. The HES momentum corresponds to the (virtual) photon energy of $\omega = E_e - E_{e'} = 1.5$ GeV where the production-cross sections for both the $p(\gamma, K^+)\Lambda$ and the $p(\gamma, K^+)\Sigma^0$ reactions are large. The virtual photons are emitted at the angle of $\theta_{e\gamma^*} = 3.9^\circ$ as a central angle to be accepted by HES is at $\theta_{ee'} = 8^\circ$ with respect to the incident beam direction. On the other hand, the central angle of the scattered particle in HKS is $\theta_{eK^+} = 15^\circ$. It is noted that the virtual photons are emitted to the HKS side because a scattering plane (plane defined by ee') and a reaction plane (plane defined by γ^*K^+) is in (anti)parallel for our setup. Therefore, the K^+ scattering angle with respect to the virtual photon is at $\theta_{\gamma^*K^+}^{\text{lab.}} = \theta_{eK^+} - \theta_{e\gamma^*} = 11.1^\circ$ in the laboratory frame. Figure 3 shows a predicted differential cross section for the ${}^{12}\text{C}(\gamma, K^+)_{\Lambda}^{12}\text{B}$ reaction at $\omega = 1.1$ GeV [47]. The differential cross section for the hypernuclear production is larger

at the smaller K^+ scattering angle. HKS is set to cover as small K^+ scattering angle as possible

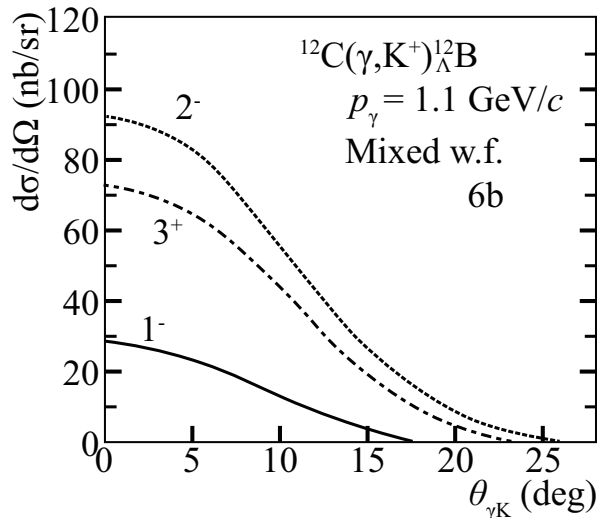


FIG. 3. Theoretical calculation for the differential cross section of the (γ, K^+) reaction as a function of the K^+ scattering angle [47]. The cross section becomes larger as the scattering angle gets smaller.

avoiding a physical interference with other components such as a beam line for unused beams and Bremsstrahlung photons generated in the target. The kinematic parameters of the experiment are summarized in Tab. I. One can notice that a square of the four-momentum transfer with the negative sign $Q^2 = -q^2$ is small, and thus, the virtual photon may be almost treated as a real photon.

The momentum acceptance for HES and HKS is shown in Fig. 4. We set the central momentum of HKS at 1.2 GeV/c to measure events of Λ and Σ^0 via the $p(e, e'K^+)$ reaction as well as the hypernuclear events with the same spectrometer setting. One of notable advantages of our experiment is a capability of an accurate calibration of the absolute binding energy by using the Λ and Σ^0 productions. Uncertainties of the known masses of Λ and Σ^0 are only 6 and 24 keV/c², respectively. In addition, events of the $p(e, e'p)\eta'$ reaction would be useful for the check of the energy calibration.

B. Particle detectors

HES has two drift chambers (EDC1 and 2) and two layers of plastic scintillation counters (ETOF1 and 2) as shown in Fig. 5. On the other hand, HKS has two types of Cherenkov counters (WC and AC) for a particle identification in addition to drift chambers (KDC1 and 2) and TOF counters (KTOF 1X, 1Y and 2X). All of the detectors were used in the previous hypernuclear

TABLE I. Summary of the kinematics parameters in the proposed experiment.

Item	Value	
Beam (e)	Energy (/GeV) (Required) energy spread and drift	2.24 1×10^{-4} (FWHM)
PCS + HES (e')	Central momentum $p_{e'}^{\text{cent.}}$ [/(GeV/c)] Central angle $\theta_{e'e'}^{\text{cent.}}$ Solid angle acceptance $\Omega_{e'}$ (/msr) (at $p_{e'}^{\text{cent.}}$) Momentum resolution $\Delta p_{e'}/p_{e'}$	0.74 8° 3.4 4.4×10^{-4} (FWHM)
PCS + HKS (K^+)	Central momentum $p_{K^+}^{\text{cent.}}$ [/(GeV/c)] Central angle $\theta_{eK^+}^{\text{cent.}}$ Solid angle acceptance Ω_{K^+} (/msr) (at $p_{K^+}^{\text{cent.}}$) Momentum resolution $\Delta p_{K^+}/p_{K^+}$	1.2 15° 8.3 2.9×10^{-4} (FWHM)
$p(e, e'K^+)\Lambda$	$\sqrt{s} = W$ (/GeV) Q^2 [/(GeV/c) 2] Recoil momentum q_Λ [/(GeV/c)] K^+ scattering angle wrt virtual photon, $\theta_{\gamma^*K^+}$ ϵ ϵ_L	1.914 0.032 0.46 11.1° 0.59 0.008

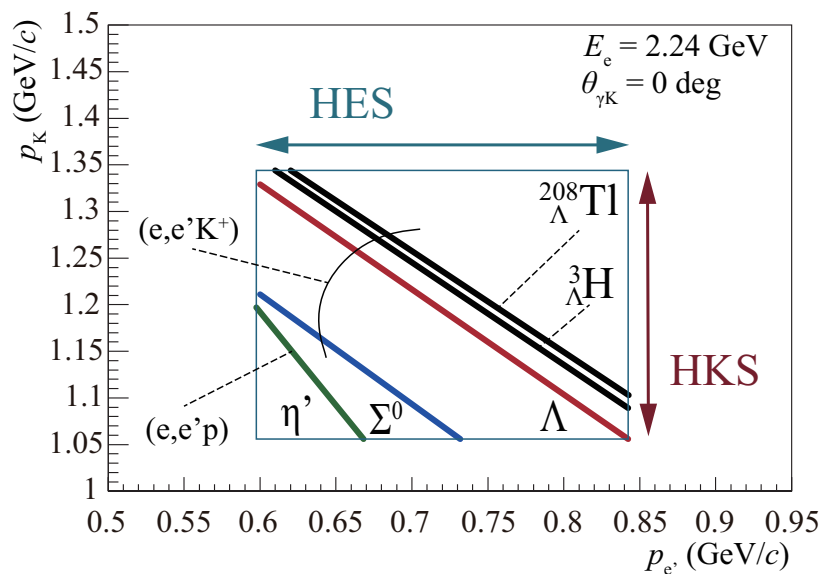


FIG. 4. Momentum acceptance of HES and HKS in the proposed experiment. It covers Λ and Σ^0 productions from a proton target as well as the hypernuclear productions. Expected kinematics lines for ${}^6_\Lambda\text{He}$, ${}^9_\Lambda\text{Li}$, and ${}^{11}_\Lambda\text{Be}$ are between the lines for ${}^3_\Lambda\text{H}$ and ${}^{208}_\Lambda\text{Tl}$.

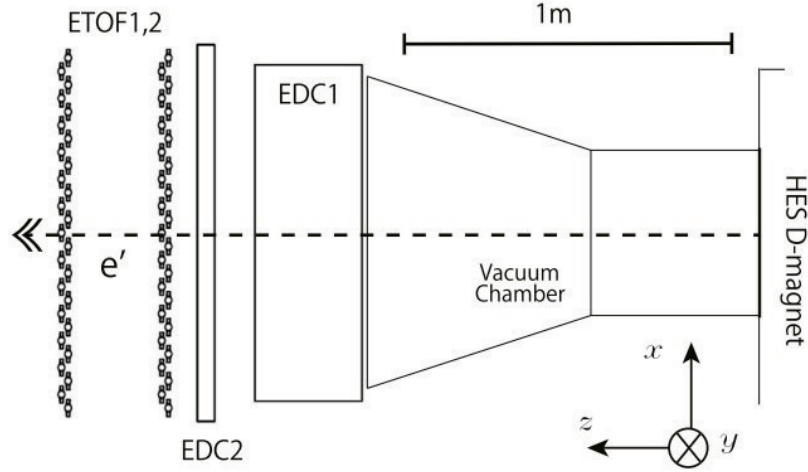


FIG. 5. Schematic of HES detectors.

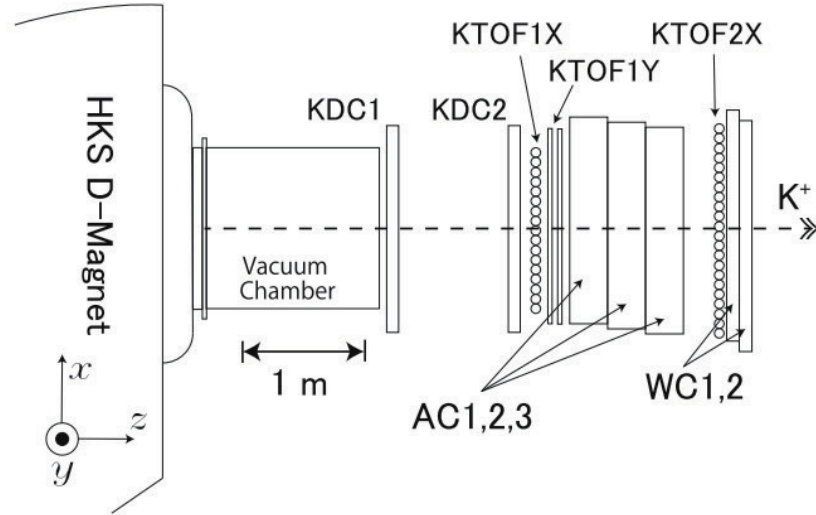


FIG. 6. Schematic of HKS detectors.

experiment at Hall C except for WC. Reflection sheets attached to inner surfaces of the WC containers were found to be partially fallen off. Therefore, we need new water containers for WC. The new containers were designed and tested in Japan, and it was found that the new WC has a much better capability to reject protons due to a doubled yield of Cherenkov light compared to the former one. The new WC containers are planned to be transported to JLab by the end of 2023. Signal checks and commissioning for other detectors by using cosmic rays are in progress at JLab. For example, cosmic-ray tests in which the yield of the number of photoelectrons (NPEs) for MIP particles was measured and checked for each segment of AC were completed in 2022. We are going to start the signal checks for the TOF counters and the drift chambers.

C. Experimental targets

Isotopically enriched materials of ${}^6\text{Li}$, ${}^9\text{Be}$, and ${}^{11}\text{B}$ with the areal density of 100 mg/cm^2 are used as nuclear targets. The experimental targets are mount on a target ladder, and are alternately exposed to the electron beam by changing the ladder position.

D. Trigger rate

Particle rates in HES and HKS are estimated based on data taken in the previous experiment E05-115. Table II shows the estimated rates for the beam currents of 50 and $30\ \mu\text{A}$. The counting

TABLE II. Expected counting rates in HES and HKS with assumptions that the signal widths for the coincidence are 30 and 200 ns for HES and HKS, respectively. Accidental coincidence rates are shown in the last column. It is noted that the Cherenkov counters do not participate in the estimation.

Beam current ($/\mu\text{A}$)	Target [$/(mg/cm^2)$]	Rate ($/\text{kHz}$)				
		HES	HKS		Coincidence btw HES and HKS	
		e'	K^+	π^+		p
50	${}^6\text{Li}$	120	0.27	22	28	1.0
	${}^9\text{Be}$ (100)	140	0.26	21	27	1.8
	${}^{10}\text{B}$	170	0.25	21	26	2.1
30	${}^6\text{Li}$	73	0.16	13	17	0.5
	${}^9\text{Be}$ (100)	81	0.15	13	16	0.5
	${}^{10}\text{B}$	100	0.15	12	16	0.3

rate in HES is smaller by an order of magnitude as the e' scattering angle $\theta_{ee'}$ is larger compared to that in E05-115. In addition, positrons which were generated in the target and emitted at the forward angle with the relatively smaller momentum were transported to the downstream of the HKS dipole magnet. The positrons did not hit particle detectors directly, but, in the vacuum chamber that was attached to the HKS dipole magnet (Fig. 6), generated secondary particles to be detected by the HKS detectors. The proposed experiment is designed not to suffer from the positron background by using PCS instead of a simple dipole magnet (splitter magnet; SPL). Therefore, the counting rate in HKS is expected to be smaller as well. The expected rate for the accidental coincidence between HES and HKS for each target is shown in the last column of Tab. II. The accidental coincidence rate was evaluated with an assumption that signal widths for the coincidence are 200 and 30 ns for HKS and HES, respectively. The Cherenkov counters

do not participate in the estimation. The accidental coincidence rate is up to a few kHz for the beam-current condition of $50 \mu\text{A}$ whereas a data acquisition system is expected to tolerate with a trigger rate of a few 10 kHz. Therefore, the DAQ should not be an issue.

IV. EXPECTED RESULTS

A. Yield and background estimation

An yield of hypernucleus N_{HYP} was evaluated by the following equation:

$$N_{\text{HYP}} = \left(\frac{d\sigma}{d\Omega_K} \right) \times \Omega_K \times N_{\text{target}} \times N_{\text{VP}} \times \epsilon \quad (1)$$

where $N_{\text{target,VP}}$ are the numbers of target nuclei and incident virtual photons, and Ω_K is the solid angle of HKS. $\left(\frac{d\sigma}{d\Omega_K} \right)$ is the differential cross section for the (γ, K^+) reaction. $\epsilon (= 19\%)$ is a total efficiency which takes into account efficiencies of the particle tracking, K^+ selection by Cherenkov counters, DAQ, as well as a K^+ decay factor of 0.295. The number of virtual photons N_{VP} was obtained by

$$N_{\text{VP}} = \Gamma^{\text{HES}} \times N_{\text{beam}} \quad (2)$$

where $\Gamma^{\text{HES}} (= 6.66 \times 10^{-6} \text{ /electron})$ is the integrated virtual photon flux evaluated by an integration over the HES acceptance in the Monte Carlo simulation based on Geant4. The expected yield per day for each target is summarized in Tab III.

TABLE III. Expected yields of hypernuclei.

Reaction	Target thickness [/(g/cm ²)]	Beam current (/ μA)	Assumed cross section [/(nb/sr)]	Yield per day
${}^6\text{Li}(e, e' K^+)_{\Lambda}{}^6\text{He}$	100	50	10	24
${}^9\text{Be}(e, e' K^+)_{\Lambda}{}^9\text{Be}$			7.6	12
${}^{11}\text{B}(e, e' K^+)_{\Lambda}{}^{11}\text{B}$			30	39

A simple Monte Carlo simulation was performed to determine a necessary beam time for each experimental target. The goal of statistical uncertainty is $|\Delta B_{\Lambda}^{\text{stat.}}| = 40 \text{ keV}$. By the 0.6-MeV resolution in FWHM, 40 counts of signals would be enough to achieve the goal uncertainty if there are no backgrounds. However, it is expected that there are background events under the signal events as shown in Fig. 7. There are two dominant sources of the background events:

(1) an accidental coincidence between HES and HKS, and (2) a quasi-free Λ production (QF). The horizontal axis of the figure is the Λ binding energy with the negative sign,

$$-B_{\Lambda} = M_{\text{HYP}} - (M_{\Lambda} + M_{\text{core}}) \quad (3)$$

where $M_{\text{HYP,core},\Lambda}$ are the masses of a hypernucleus, a core nucleus, and a Λ . In the experiment, the hypernuclear mass M_{HYP} is derived by measuring momentum vectors of e' and K^+ in HES and HKS, respectively. Bound hypernuclear states locate at $-B_{\Lambda} < 0$ MeV whereas the QF-

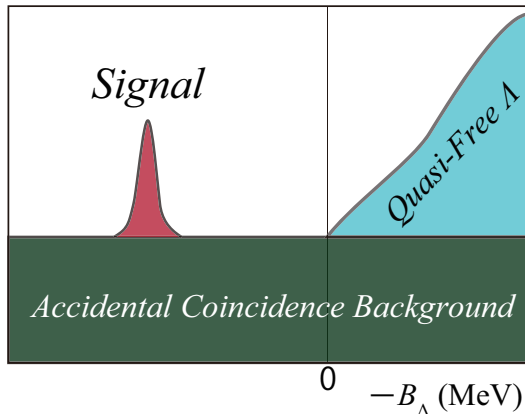


FIG. 7. Schematic of the signal of hypernuclear production, the accidental coincidence background, and the background from quasi-free Λ production.

background events are in the region of $-B_{\Lambda} \geq 0$ MeV. Therefore, particularly the accidental coincidence events need to be taken into account to determine the required beam time. The accidental coincidence background in the binding-energy spectrum was evaluated based on the result of previous experiment E05-115 and the expected counting rates in HES and HKS in the proposed experiment are shown in Tab. II. It is worth noting that the estimation of the counting rates in the spectrometers fairly agrees with those in the previous experiment E05-115.

Figure 8 shows a flow chart of the simulation in which the necessary beam time was estimated. At first, a simulated spectrum was generated. The assumed differential cross sections and the amount of QF background were based on theoretical predictions and the previous measurements [16, 17, 48]. The accidental background distribution was assumed to be flat. Mixed event analysis (MEA) in which random combinations between e' and K^+ are used to evaluate the shape of the accidental background with higher statistics is used for the real experiment. The binding energy spectrum is subtracted by the accidental background distribution evaluated by MEA for the final spectral fit. To simulate the accidental background distribution obtained by the MEA technique,

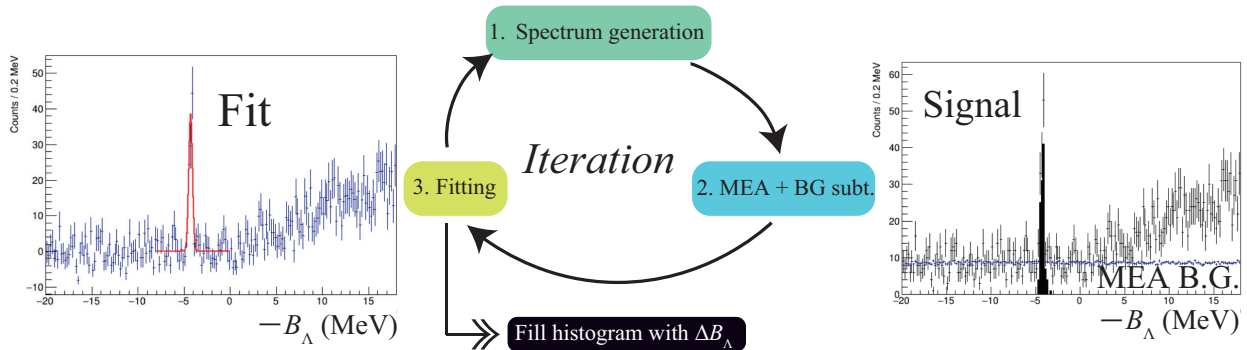


FIG. 8. Flow chart of the simulation to evaluate the required beam times.

the accidental background events were generated with higher statistics by a factor of 100 and the whole spectrum of the accidental background was scaled by a factor of 1/100. Then, the scaled distribution, which corresponds to the accidental background distribution obtained by MEA in the real data analysis, was subtracted from the original spectrum, followed by the spectral fit to the signal events. The statistical uncertainty $\Delta B_{\Lambda}^{\text{stat.}}$ obtained by the spectral fit was filled in a histogram. The simulation was iterated 1000 times for each condition.

Figure 9 shows the $\Delta B_{\Lambda}^{\text{stat.}}$ obtained by the simulation for the ${}^6\text{Li}(e, e'K^+)_{\Lambda}{}^6\text{He}$ reaction in cases of 3, 5, 10, and 15 days of beam time. The statistical uncertainty tends to be smaller as the beam time get longer. The mean values ($\mu_{\Delta B}$) and standard deviations ($\sigma_{\Delta B}$) of the $\Delta B_{\Lambda}^{\text{stat.}}$ distributions are plotted in Fig. 10. We took the beam time that fulfills a condition of $\mu_{\Delta B} + \sigma_{\Delta B} \leq 40$ keV as the required beam time. As a result, the necessary beam times to achieve the goal uncertainty are seven and five days in the cases of 30- and 50- μA beam currents, respectively, for the ${}^6\text{Li}(e, e'K^+)_{\Lambda}{}^6\text{He}$ reaction. The simulation was performed for the other reactions as well. The required beam time for each target is shown in Tab. IV.

TABLE IV. Required beam time to achieve the goal of statistical error $|\Delta B_{\Lambda}^{\text{stat.}}| = 40$ keV for the beam-current conditions of $I_{\text{beam}} = 30$ and $50 \mu\text{A}$.

Reaction	Assumed cross section [/(nb/sr)]	Necessary beam time (/days)		Ratio [$t(I_{\text{beam}}^{50})/t(I_{\text{beam}}^{30})$] ($\times 1.7$)
		$I_{\text{beam}}^{30} = 30 \mu\text{A}$	$I_{\text{beam}}^{50} = 50 \mu\text{A}$	
${}^6\text{Li}(e, e'K^+)_{\Lambda}{}^6\text{He}$	10	7	5	$\times \frac{1}{1.4} = 0.71$
${}^9\text{Be}(e, e'K^+)_{\Lambda}{}^9\text{Li}$	7.6	19.5	14	
${}^{11}\text{B}(e, e'K^+)_{\Lambda}{}^{11}\text{Be}$	30	3.5	2.5	

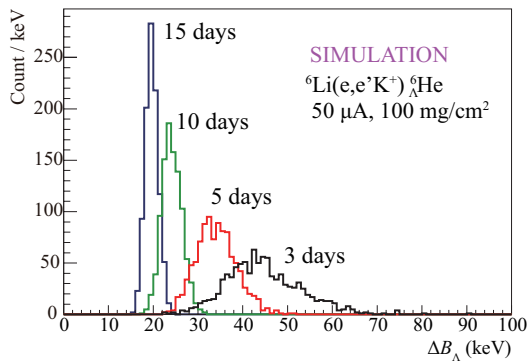


FIG. 9. Statistical uncertainties ($\Delta B_{\Lambda}^{\text{stat.}}$) obtained in the simulation for the ${}^6\text{Li}(e, e'K^+){}^6_{\Lambda}\text{He}$ reaction. The assumed beam current and target thickness are $50 \mu\text{A}$ and 100 mg/cm^2 , respectively. Peak fits to simulated spectra were performed 1000 times for each beam-time condition (3, 5, 10, and 15 days), and the obtained statistical uncertainties are filled in the histogram.

B. Expected spectra and total accuracy

Expected spectra for the ${}^6\text{Li}(e, e'K^+){}^6_{\Lambda}\text{He}$, ${}^9\text{Be}(e, e'K^+){}^9_{\Lambda}\text{Li}$, and ${}^{11}\text{B}(e, e'K^+){}^{11}_{\Lambda}\text{Be}$ reactions are shown in Figs. 11, 12, and 13, respectively. The statistical uncertainty to determine the binding

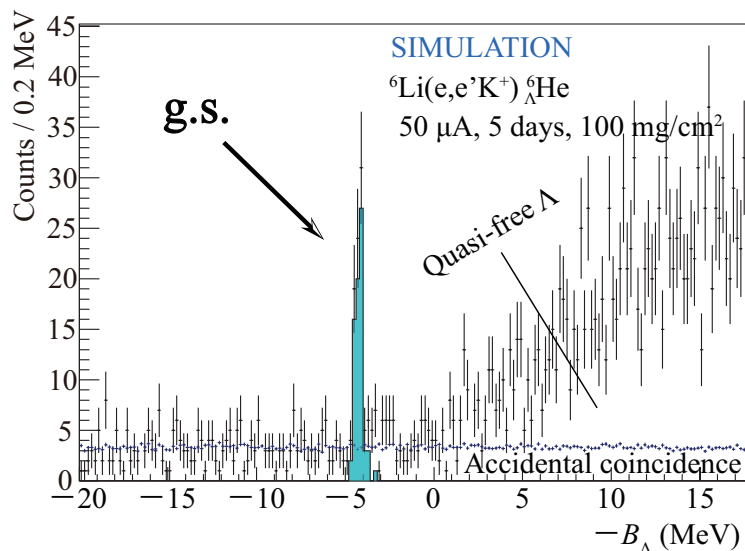


FIG. 11. Expected spectrum for the ${}^6\text{Li}(e, e'K^+){}^6_{\Lambda}\text{He}$ reaction in the proposed experiment.

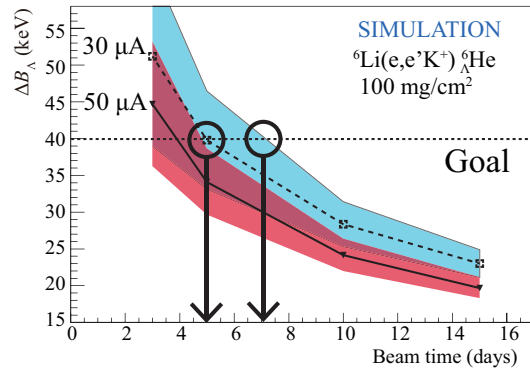


FIG. 10. Mean value of the statistical uncertainty on B_{Λ} (Fig. 9) as a function of a beam time for the ${}^6\text{Li}(e, e'K^+){}^6_{\Lambda}\text{He}$ reaction. Bands colored by blue and red correspond to standard deviations for the cases of 30- and 50- μA beam currents, respectively. Necessary beam times, which meet the goal uncertainty $|\Delta B_{\Lambda}^{\text{stat.}}| = 40 \text{ keV}$, are 5 and 7 days for the beam currents of 30 and $50 \mu\text{A}$, respectively.

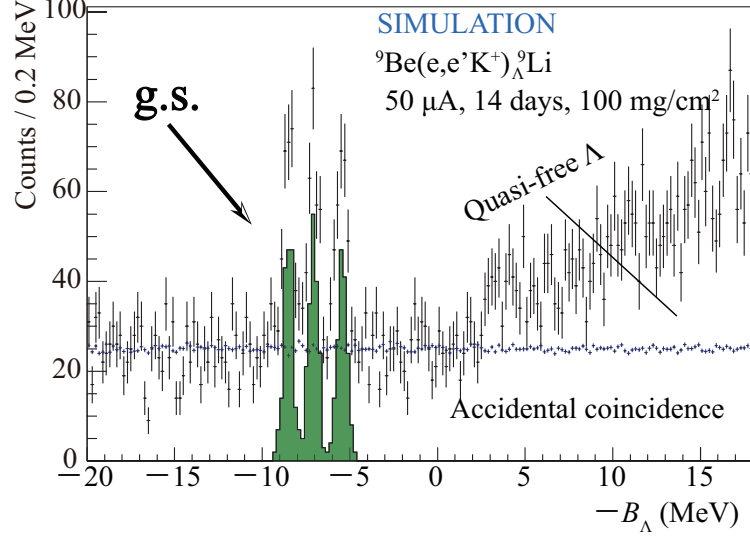


FIG. 12. Expected spectrum for the ${}^9\text{Be}(e, e'K^+){}^9\text{Li}$ reaction in the proposed experiment.

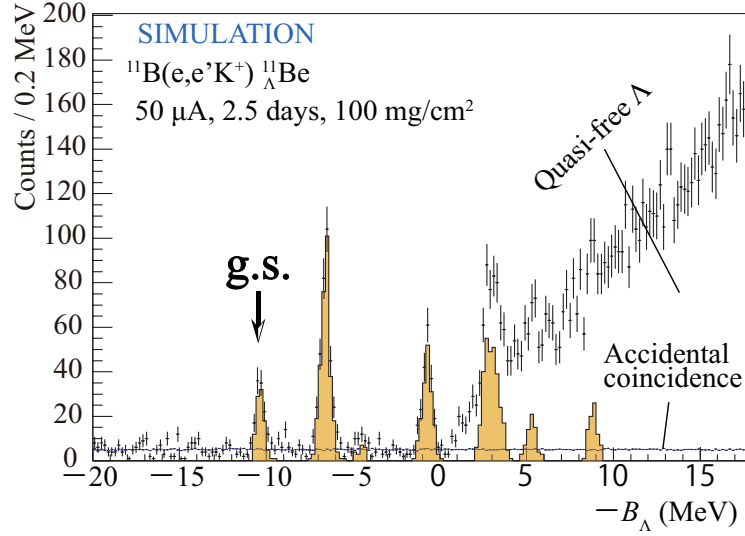


FIG. 13. Expected spectrum for the ${}^{11}\text{B}(e, e'K^+){}^{11}\text{Be}$ reaction in the proposed experiment.

energy for the ground peak is $|\Delta B_{\Lambda}^{\text{stat.}}| = 40$ keV. On the other hand, the systematic error is estimated to be $|\Delta B_{\Lambda}^{\text{sys.}}| = 55$ keV [49]. Therefore, the total error would be $|\Delta B_{\Lambda}^{\text{total}}| \leq 70$ keV if a square root of quadratic sum of the statistical and systematic errors is taken.

V. SUMMARY OF REQUESTING CONDITIONS AND BEAM TIME

A. Beam conditions

We request a 50- μ A beam at $E_e = 2.24$ GeV with a bunch frequency of 500 MHz. In order to achieve the sufficient precision in the resulting missing-mass spectrum, the beam energy spread and energy centroid are required to be $\Delta p/p \leq 1 \times 10^{-4}$ (FWHM) as was achieved in the previous hypernuclear experiments at Hall C (E05-115, 2009) [46] and A (E12-17-003: tritium experiment, 2018) [50, 51]. A beam raster with the area of about 2×2 mm² would need to be applied particularly for the ⁷Li target to avoid a damage on it.

B. Beam time

The experimental setup is the same as that for the approved experiments E12-15-008 and E12-20-013. The energy scale calibration is performed by using Λ and Σ^0 productions from the a polyethylene (CH₂) target. In addition, events that correspond to the state of ¹¹B($J^\pi = 3/2^+$; g.s.) $\otimes s_{1/2}^\Lambda$ in the ¹²C($e, e'K^+$) _{Λ} ¹²B spectrum are used for the calibration as well. The beam time for the above calibration is a part of E12-15-008, and can be shared with the proposed experiment. Therefore, in this proposal, we request only the beam time for the physics runs, which are

TABLE V. Requesting beam time of the proposed experiment. A total of 516 hours (21.5 days) is requested.

Target		I_{beam} (/ μ A)	Beam time (/hours)	Hypernucleus	Yield (g.s. peak)
Material	x_t [/(mg/cm ²)]				
⁶ Li	100	50	120	⁶ _{Λ} He	120
⁹ Be			336	⁹ _{Λ} Li	168
¹¹ B			60	¹¹ _{Λ} Be	97
Total			516		

for the ⁶Li, ⁹Be, and ¹¹B targets. Requesting beam time is shown in Tab. V. We request a total beam time of 516 hours (21.5 days).

VI. SUMMARY

The proposed experiment measures the Λ binding energies of ⁶ _{Λ} He, ⁹ _{Λ} Li, and ¹¹ _{Λ} Be hypernuclei with the accuracy of $|\Delta B_\Lambda^{\text{total}}| = 70$ keV to investigate CSB in the ΛN interaction. The beam

condition and the experimental setup are the same as those for E12-15-008 (and E12-20-013) in which existing spectrometers HES and HKS are used at Hall C. Energy-calibration data which are planned to take in E12-15-008 are commonly used. Therefore, a total of the requesting beam time is 516 hours (21.5 days), which is only for the physics runs, in the proposed experiment. This experiment leads to a completion of the p-shell hypernuclear data up to the mass number of twelve to pin down the origin of CSB by combining complementary experiments by hadron beams at J-PARC.

-
- [1] K. Miwa *et al.*, *Phys. Rev. Lett.* **128**, 072501 (2022).
 - [2] T. Nanamura *et al.*, *Prog. Theor. Exp. Phys.* **2022**, 9, 093D01 (2022).
 - [3] J. W. Price *et al.*, *AIP Conf. Proc.* **2130**, 020004 (2019).
 - [4] K. Miwa *et al.*, Proposal to J-PARC, P86 (2021).
 - [5] S.N. Nakamura *et al.*, Proposal to JLab, E12-15-008 (2015).
 - [6] F. Garibaldi *et al.*, Proposal to JLab, E12-20-013 (2020).
 - [7] A. Esser *et al.* (A1 Collaboration), *Phys. Rev. Lett.* **114**, 232501 (2015).
 - [8] F. Schulz *et al.* (A1 Collaboration), *Nucl. Phys. A* **954**, 149 (2016).
 - [9] T.O. Yamamoto *et al.*, *Phys. Rev. Lett.* **115**, 222501 (2015).
 - [10] T. Gogami *et al.*, Proposal to JLab, E12-19-002 (2019, 2020, and 2021).
 - [11] T. Gogami *et al.*, *AIP Conf. Proc.* **2319**, 080019 (2021).
 - [12] T. Gogami *et al.*, *EPJ Web Conf.* **271**, 01001 (2022).
 - [13] H. Tamura *et al.*, Proposal to J-PARC, E63 (2016).
 - [14] H. Tamura *et al.*, *JPS Conf. Proc.* **17**, 011004 (2017).
 - [15] S.N. Nakamura *et al.* (HKS (JLab E01-011) Collaboration), *Phys. Rev. Lett.* **110**, 012502 (2013).
 - [16] T. Gogami *et al.* (HKS (JLab E05-115) Collaboration), *Phys. Rev. C* **94**, 021302(R) (2016).
 - [17] T. Gogami *et al.* (HKS (JLab E05-115) Collaboration), *Phys. Rev. C* **93**, 034314 (2016).
 - [18] O. Hashimoto and H. Tamura, *Prog. Par. Nucl. Phys.* **57**, 2, 564–653 (2006).
 - [19] M. Juric *et al.*, *Nucl. Phys. B* **52**, 1–30 (1973).
 - [20] D. H. Davis, *Nucl. Phys. A* **754**, 3–13 (2005).
 - [21] E. Botta, T. Bressani A. Feliciello, *Nucl. Phys. A* **960**, 165–179 (2017).
 - [22] S. B. Yang *et al.* (J-PARC E13 Collaboration), *Phys. Rev. Lett.* **120**, 132505 (2018).
 - [23] L. Tang *et al.* (HKS (JLab E05-115 and E01-011) Collaborations), *Phys. Rev. C* **90**, 034320 (2014).
 - [24] T. Gogami *et al.* (HKS (JLab E05-115) Collaboration), *Phys. Rev. C* **103**, L041301 (2021).
 - [25] P Eckert *et al.*, *EPJ Web Conf.* **271**, 01006 (2022)
 - [26] P. Klag *et al.*, *Nucl. Instrum. Methods, Phys. Res. Sect. A* **910**, 1, 147–156 (2018).
 - [27] P. Klag *et al.*, *J. Phys.: Conf. Ser.* **2482**, 012016 (2023).

- [28] C. Rappold *et al.*, *Phys. Lett. B* **728**, 543–548 (2014).
- [29] The ALICE Collaboration, *Phys. Lett. B* **797**, 134905 (2019).
- [30] The STAR Collaboration, *Nat. Phys.* (2020); <https://doi.org/10.1038/s41567-020-0799-7>.
- [31] P. Liu, *Nucl. Phys. A* **982**, 811–814 (2019).
- [32] S. Acharya *et al.*, *Nature* **588**, 232 (2020).
- [33] Y. Kamiya *et al.*, *Phys. Rev. C* **105**, 014915 (2022).
- [34] T. Gogami *et al.*, *Nucl. Instrum. Methods, Phys. Res. Sect. A* **817**, 70–84 (2016).
- [35] T. Gogami *et al.*, *EPJ Web Conf.* **271**, 11002 (2022).
- [36] T. Gogami *et al.*, Proposal to J-PARC, E94 (2022).
- [37] Y. Akaishi *et al.*, *Phys. Rev. Lett.* **84**, 16 (2000).
- [38] H. Nemura *et al.*, *Phys. Rev. Lett.* **89**, 14 (2002).
- [39] E. Hiyama *et al.*, *Phys. Rev. C* **80**, 054321 (2009).
- [40] E. Hiyama *et al.*, *Prog. Theor. Phys.* **128**, 105 (2012).
- [41] A. Gal, *Phys. Lett. B* **744**, 352 (2015).
- [42] E. Botta, *AIP Conf. Proc.* **2130**, 030003 (2019).
- [43] H. Le *et al.*, *Phys. Rev. C* **107**, 024002 (2023).
- [44] T. Gogami *et al.*, *Nucl. Instrum. Methods Phys. Res. Sect. A* **729**, 816–824 (2013).
- [45] Y. Fujii *et al.*, *Nucl. Instrum. Methods Phys. Res. Sect. A* **795**, 351–363 (2015).
- [46] T. Gogami *et al.*, *Nucl. Instrum. Methods Phys. Res. Sect. A* **900**, 69–83 (2018).
- [47] T. Motoba, M. Sotona, K. Itonaga *et al.*, *Prog. Theor. Phys. Suppl.* **117**, 123–133 (1994).
- [48] A. Umeya, Presentation in the international workshop BISHOP2023, Rez, Czech Republic, May 17, 2023.
- [49] T. Toyoda, *Master's Thesis*, Kyoto University, Kyoto, Japan, 2021 (in Japanese).
- [50] K. N. Suzuki, T. Gogami *et al.*, *Prog. Theor. Exp. Phys.* **2022**, 1, 013D01 (2022).
- [51] B. Pandey, L. Tang *et al.* (Hall A Collaboration), *Phys. Rev. C* **105**, L051001 (2022).